Proceedings of the Institute of Acoustics

THE NON-LINEAR OSCILLATIONS OF MULTIPLE BUBBLES IN A SIMULATED ACOUSTIC FIELD.

T. G. Leighton, M. Adlam, A. J. Walton, J. E. Field.

Cavendish Laboratory, Madingley Road, Cambridge CB3 OHE

1. ABSTRACT

Gas bubbles in liquids are capable of forced oscillations in a sound field. Photographic study of these non-linear oscillations is difficult. It is technically most feasible at low acoustic frequencies, where lower framing rates are required, and where the resonance bubble size is larger. However, the acoustic pressures required to elicit a nonlinear response from the bubble might, if generated at audible frequencies, be damaging to the hearing. This paper outlines an experimental solution to the problem, whereby a volume of liquid containing bubbles of a size which can be readily photographed, is vibrated vertically. The oscillating pressure in the water mimics an acoustic field at the vibration frequency, and the bubble responds to it as such. The apparatus has minimal audible emissions, yet the oscillating pressure is of such an amplitude as to generate highly nonlinear oscillations in the bubble. The experiment provides a good example of forced oscillation, as well as illustrating a subtle solution to a difficult experimental problem. Radius-time data from a given bubble were obtained using high-speed and stroboscopic photography, and were compared with the numerical predictions obtained from the Rayleigh-Plesset equation.

2. INTRODUCTION

A spherical gas bubble within a liquid may perform volume pulsations. Given a mechanical exciting impulse, the amplitude of oscillation of the bubble wall will be small, and so the bubble will approximate to a linear oscillator. The pulsations will occur at a well-defined resonance frequency ν_r, where

$$\nu_r = (1/2\pi R_o).\sqrt{(3\kappa P_o/\rho)} \ , \qquad (1)$$

where R_o is the equilibrium bubble radius, ρ is the liquid density, P_o is the ambient hydrostatic pressure and κ is the so-called polytropic index (which takes a value between unity and γ depending on whether the gas is behaving isothermally, adiabatically, or in some intermediate manner) [1]. For air bubbles in water, equation 1 reduces to

$$\nu_r \, . \, R_o \approx 3 \ hertz. \ metres \ . \qquad (2)$$

The acoustic output of such a bubble is typically an exponentially-decaying sinusoid [2]. The gas bubble may be subjected to a periodic driving force in the form of an acoustic wave, which can give rise to nonlinear oscillations in the bubble, the amplitude of oscillation of the bubble wall now being higher. Such acoustic activation of gas bubbles in liquid is of importance in two general fields: medical ultrasound, and underwater communications. The former employs acoustic frequencies of order MHz, whilst the latter uses kHz. From equation 2, it can be seen that the bubble radii resonant with these frequencies are of magnitude 10^{-6} m and 10^{-4} m respectively. Due to the small size and rapid motions of these bubbles, it is very difficult to image them directly. As a result, much use is made of numerical methods to predict the oscillatory motion of these bubbles. One of the most common of these is the Rayleigh-Plesset (or RPNNP) equation for a single bubble in an infinite medium:

$$R\ddot{R}+3\dot{R}^2/2 = (1/\rho)\{(P_o + 2\sigma/R_o - P_v)(R_o/R)^{3\kappa} - 2\sigma/R - 4\mu\dot{R}/R - P_o - P(t)\}, \qquad (3)$$

where R is the bubble radius, R_o its equilibrium value, σ, ρ and μ are respectively the surface tension, density and viscosity of the liquid, P_o the hydrostatic pressure, $P(t)$ the time-varying pressure component (ie. the driving term), P_v is the vapour pressure within the bubble. When the surface tension and viscosity terms in the Rayleigh-Plesset equation are deemed negligible, and $P(t)$ set to zero, the formulation approximates to the resonant oscillations of an unforced bubble, at a frequency ν_r given by equation 1. The Rayleigh-Plesset equation assumes: a) sphericity of the bubble; b) spatially uniform conditions inside the bubble; c) the bubble radius is small compared with the acoustic wavelength; d) no body forces (eg. gravitational) are present; e) bulk viscous effects can be ignored; f) the density of

the liquid is large, and its compressibility is small, compared with the values for the gas within the bubble; g) the gas content of the bubble is constant; h) the vapour pressure is constant during the oscillation [3]. These assumptions limit the applicability of the equation.

The aim of this study was to construct a model system that would enable the simultaneous study of several bubbles in a low-frequency acoustic field. The Rayleigh-Plesset predictions could be tested against experimental data derived from high-speed photography. Bubbles of air, helium and propane were used to test the dependence of the oscillation on the polytropic index.

3. EXPERIMENTAL

The acoustic field was generated in a non-inertial frame from the pressure fluctuations in a vibrated fluid. A cell containing fluid was oscillated vertically (figure 1). The pressure P at depth h below the liquid surface oscillates as a result of the oscillating weight of the liquid column above it. If the displacement of the column is $y=A\sin\omega t$ then the acceleration of the cell is $\ddot{y}= -\omega^2 A\sin\omega t$ .If the liquid column is prismatic, with cross-sectional surface area s, then the net upward force on the column is $(Ps-P_o s-\rho hg)$. Since the mass of the column is ρhs, then from Newton's second law,

$$(P-P_o)s - \rho hgs = \rho hs.(-\omega^2 A\sin\omega t) . \quad (4)$$

The pressure at the base of the column is therefore

$$P = (P_o + \rho hg) - (\rho h\omega^2 A\sin\omega t) . \quad (5)$$

This expression corresponds to an oscillating pressure of amplitude $(-\rho h\omega^2 A)$ and frequency ω, superimposed on a static pressure of $(P_o+\rho hg)$. Since the latter term tends to suppress bubble oscillation, whilst the former promotes it, then large nonlinear effects are promoted if the pressure head above the liquid is reduced. Thus the vertical oscillation of a liquid can produce an intense oscillating pressure field at audio frequencies without causing discomfort. The column was vibrated at 103 Hz and the cavitation recorded with high-speed photography, the low acoustic frequency allowing sufficient data points to be taken per cycle to satisfy the Nyquist criterion. Also, the resonance bubble radius is larger (equation 1), reducing the need for high optical magnification.

The apparatus is shown in figure 2. Details are given elsewhere [4], where a study was made of isolated bubbles. The cell, made of PMMA and aluminium, has internal dimension 90 mm long and 27 mm diameter. It contains the test liquid to level 3/4, and is placed upon a vibrator (Goodmans Industries type 390). The gas head above the liquid is pumped down to about 1 Torr. Extended springs attached to the top of the cell pull up against its weight, so that at rest the cell lies at the equilibrium position of the vibrator. Without these springs, the vibrator bottoms out at high amplitude, and the motion ceases to be sinusoidal. The sinusoidal nature of the motion can be checked by illuminating the cell with a stroboscope tuned to the vibration frequency, and then plotting the cell displacement against the phase delay of the stroboscope. The vibrator is driven by an electrical sinusoid at 103 Hz from a Brookdeal Signal Source (type 471), which was amplified by a Quad 510 power amplifier. A voltmeter could be used to check signal reproducibility.

The photography was achieved with a Hadland Hyspeed rotating prism camera, operating at 2000 frames per second (fps), which had a field of view of 4 mm x 6 mm. Two 800 W "red-head" spotlights, used together with a 250 W source, provided illumination, a white screen being used as a diffuser. Cine film (16 mm, 400 ASA) was used in 100-foot reels, taking a few seconds of continuous photography. They were developed in ID11 at 20°C for 12 minutes. An internal strobe spot-marked the film with an accurate timing light to record on the film itself the instantaneous framing rate.

In the earlier study [4], a slow and steady stream of bubbles was introduced into the cell through a syringe in an attempt to produce a bubble of a given size in an approximately isolated state. The oscillations of this bubble were then examined in isolation. In the present experiment, a higher number density of bubbles of varying size was

THE NON-LINEAR OSCILLATIONS OF MULTIPLE BUBBLES IN A SIMULATED ACOUSTIC FIELD.

employed. The stationary cell contained glycerol and was pumped down to around 1 Torr, and bubbles injected into the cell by the suction of gas through a hyperdermic needle which pierced the bung in the side of the cell (figure 2). When the required number density of bubbles had been achieved, the needle was withdrawn into the bung and the flow of gas through it ceased. The subsequent buoyant rise of the bubbles in glycerol was slow, allowing adequate time for the photography. In water, the rapidity of the buoyant rise made the above injection method unsatisfactory. Therefore the bubble population was generated by the growth of bubbles once insonation had begun through the process of rectified diffusion [5]. As well as air, bubbles of helium and propane were studied in glycerol. The liquid was left under reduced pressure overnight to degas it, and then the gas bubbles were introduced through the hyperdermic.

When a film was taken, the camera was initially started whilst the vibrator was stationary. This allowed the bubbles to be photographed whilst non-oscillatory, permitting their equilibrium radii to be subsequently measured. After a few moments, the vibrator was started. The bubble motion therefore is that of an initially stationary bubble suddenly subjected to an oscillatory pressure field, and so the boundary conditions in the numerical solution are that at $t=0$, $R=R_0$ and $\{dR/dt\}=0$. Once the film had been developed, it could be projected onto a screen. The camera lens system, along with the projection, provided a linear magnification of 100x. The cine camera enabled frame-by-frame analysis of the film to provide data for the bubble radius as a function of time. This was then be compared with the computer predictions. Only spherical bubbles were sized. The time t after the start of insonation could be measured directly since the bubble had been in the field of view at $t=0$.

Figure 1

Schematic diagram of the vibrating cell. The forces upon a liquid column are shown.

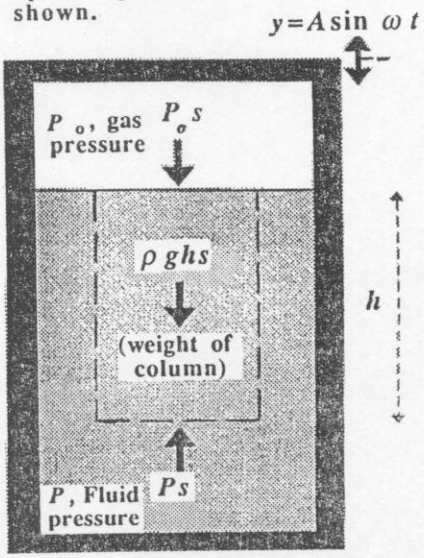

Figure 2

The apparatus used to simulate the sound field.

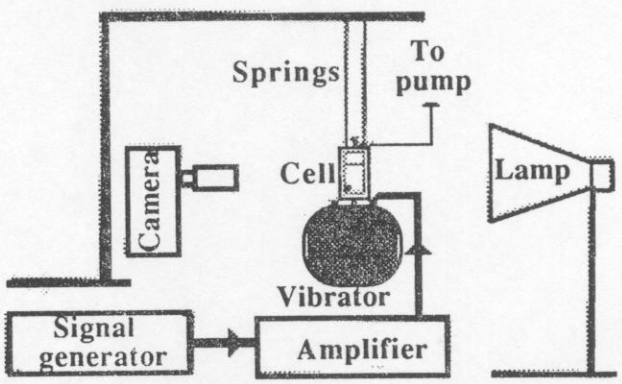

The effective pressure amplitude (the term $(\rho A w^2 h)$ in equation 5) was found in two ways [4]. Firstly, each of the parameters in the expression was directly measured, enabling the product to be calculated. Secondly, the top of the cell could be removed (so therefore the system would no longer be under reduced pressure) and a hydrophone (Bruel and Kjaer type 8103) inserted into the liquid to measure the pressure amplitude directly. To check that there was no electromagnetic pickup by the hydrophone, this measurement was performed in the absence of the test liquid: no signal was seen, proving the previous measurement of pressure amplitude genuine. A typical hydrophone trace is shown in figure 3. The acoustic amplitude took around 250 ms to reach 90% of its final value (the sound pressure data for the Rayleigh-Plesset predictions was taken at the time corresponding to the photography). A transient spike in the acoustic signal was detected approximately 20 ms after the vibrator was first switched on. To minimise the effect this limitation of the apparatus might have on the bubble oscillations, measurements of bubble radii commenced some 50 ms after the initial activation of the vibrator. In this way, the validity of a comparison between the photographic data and the Rayleigh-Plesset predictions was maintained. The bubble measurements were usually taken for 100 consecutive frames (i.e. 50 ms).

The bubbles studied had equilibrium radii from around 0.1 mm to 0.5 mm (corresponding to resonance frequencies for air bubbles in glycerol from 900 Hz to 180 Hz, and in water from 2 kHz to 400 Hz). Therefore the bubbles observed were all driven at frequencies below their resonance. The vibrator was not powerful enough to drive the bubbles adequately at higher frequencies.

4. RESULTS

Figures 4 and 5 are frames sampled from high-speed sequences of air and helium bubbles respectively. The bubbles oscillate in glycerol under a 103 Hz sound field. In each case they grow from a minimum size to a maximum. The maximum occurs in frame 14 for air, and frame 8 for helium. This is followed by a collapse. Figure 6 shows a propane bubble oscillating in glycerol starting 50 ms (figure 6a) and 135 ms (figure 6b) after the start of insonation. In between, the form of the oscillation of the largest bubble has changed. The corresponding radius measurements are shown in figures 11c and 11d. Figure 7 shows air bubbles oscillating in water. The bubbles remain approximately spherical. In figure 8 a larger air bubble is non-spherical (since the surface tension forces are weaker). Instabilities develop as it collapses. In figure 9 two air bubbles in glycerol coalesce in frame 5. However a weakness in the lower bubble develops as the sequence progresses and in frame 15 division occurs.

Figure 10 compares photographic radius-time data with the Rayleigh-Plesset predictions for two air bubbles in glycerol. In both cases a bimodal character is evident, with the maxima at 48 ms and 67 ms being of lower amplitude than the other two, and the one at 77 ms being greater that that at 58 ms. Simultaneous data from five other air bubbles, ranging in size from R_o=0.11 mm to R_o=0.93 mm, exhibited the same behaviour. Figure 11 compares theory and experiment for propane bubbles in glycerol. In all cases the Rayleigh-Plesset shows inaccuracies in predicting the behaviour of the bubbles. An interesting feature develops in the photographic data as the equilibrium bubble size increases. In figure 11a, where R_o= 0.14 mm, the behaviour is bimodal, as discussed above. However in figure 11b (R_o= 0.19 mm) the second peak is barely apparent, with the minima at 52 ms and 71 ms almost merging with the maxima at 54 ms and 74 ms respectively. The subsequent collapses at 58 ms and 77 ms are correspondingly much sharper. In figure 11c (R_o= 0.47 mm) this process has continued so that the bubble oscillation is now at half the acoustic frequency, the only evidence of the second maximum being a perturbation in the rate of collapse at 56 ms and 75 ms. This state proves to be unstable (perhaps as a result of growth or reduction of R_o through a threshold by rectified diffusion or dissolution, respectively). Figure 11d shows experimental data from the same bubble at times of between 135 ms and 180 ms after the start of insonation. The form of the oscillation is again bimodal, but at lower frequencies than that seen with smaller bubbles in figure 11a and 11b. Figure 12 compare theory and experiment for a helium bubble of equilibrium radius 0.34 mm. In 13a, the value of κ for the numerical prediction is set to unity (corresponding to the isothermal case), whilst for 13b $\kappa=\gamma=1.66$ (adiabatic). In both cases the predictions overestimate the maximum bubble size attained.

THE NON-LINEAR OSCILLATIONS OF MULTIPLE BUBBLES IN A SIMULATED ACOUSTIC FIELD.

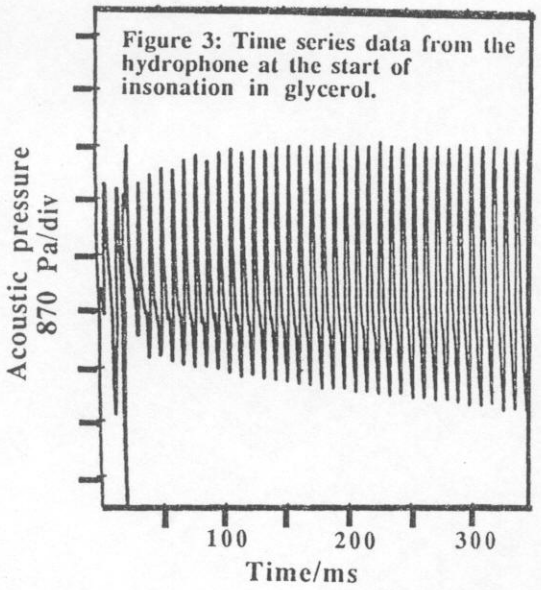

Figure 3: Time series data from the hydrophone at the start of insonation in glycerol.

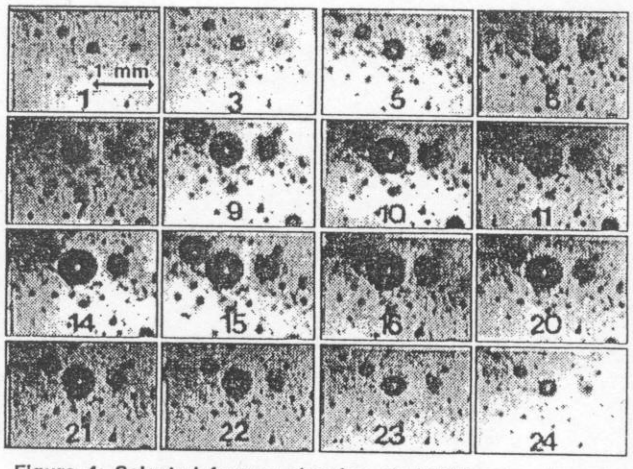

Figure 4: Selected frames showing air bubbles in glycerol. Acoustic pressure amplitude = 3050 Pa, acoustic frequency = 103 Hz, interframe time = 0.429 ms.

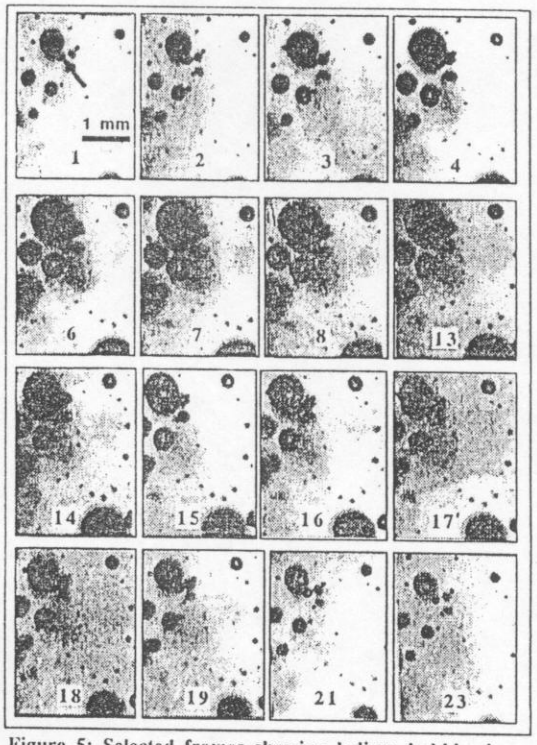

Figure 5: Selected frames showing helium bubbles in glycerol. Acoustic pressure amplitude = 4750 Pa, acoustic frequency 103 Hz, interframe time = 0.424 ms.

Figure 6: Selected frames showing propane bubbles in glycerol. Acoustic pressure amplitude=3469 Pa, acoustic frequency=103 Hz, interframe time=0.429 ms.

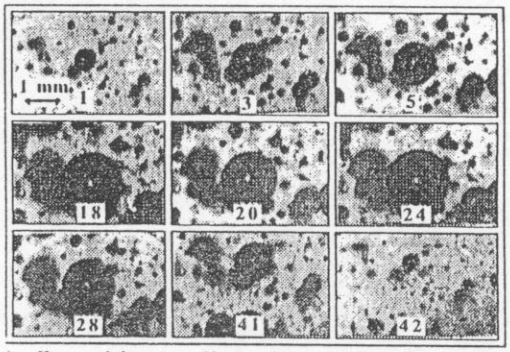

6a: Frame 1 is taken 50 ms after the start of insonation.

THE NON-LINEAR OSCILLATIONS OF MULTIPLE BUBBLES IN A SIMULATED ACOUSTIC FIELD.

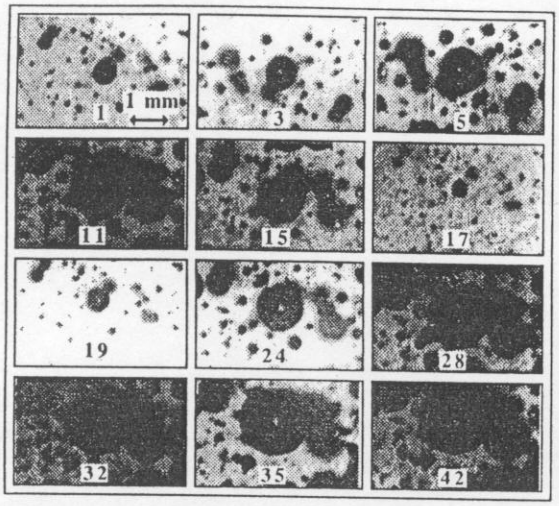

6b: Frame 1 is taken 135 ms after the start of insonation, and shows the same bubble population as 6a. The photographic data for figures 11c and 11d are taken from the largest bubble imaged here.

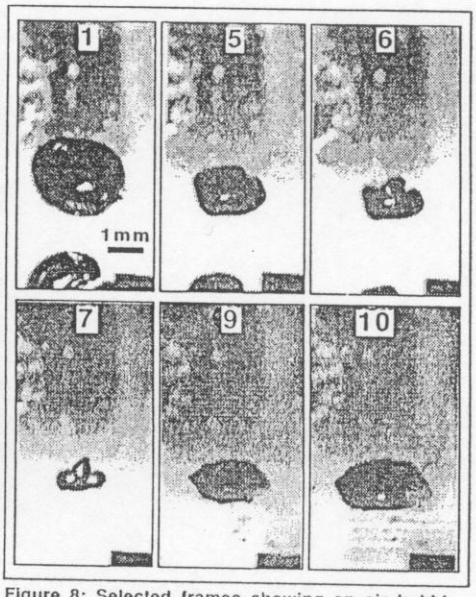

Figure 8: Selected frames showing an air bubble in water. Acoustic pressure amplitude = 1465 Pa, acoustic frequency = 103 Hz, interframe time = 0.422 ms.

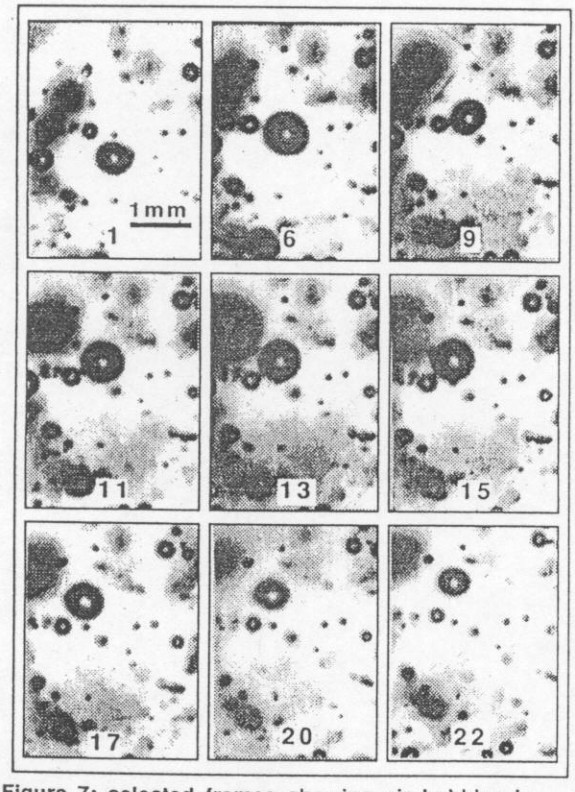

Figure 7: selected frames showing air bubbles in water. Acoustic pressure amplitude =580 Pa, acoustic frequency =103 Hz, interframe time=0.422 ms.

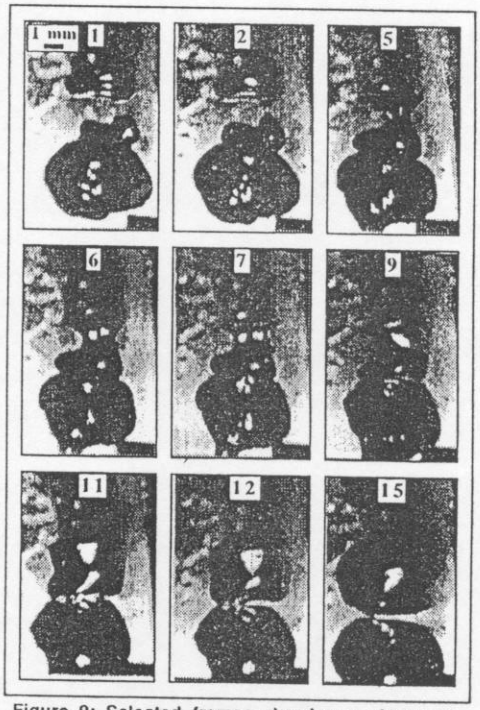

Figure 9: Selected frames showing coalescence and division of air bubbles in glycerol. Acoustic pressure amplitude = 1465 Pa, acoustic frequency = 103 Hz, interframe time = 0.429 ms.

THE NON-LINEAR OSCILLATIONS OF MULTIPLE BUBBLES IN A SIMULATED ACOUSTIC FIELD.

5. DISCUSSION

The vertically-vibrating column can simulate an acoustic field in liquid. The method of bubble generation employed in this study has several advantages over that used previously [4]. Injection of a bubble stream, as used previously [4], tends to introduce mass fluid circulation, which can rapidly draw bubbles out of the field of view of the camera, and which can force liquid into the pumping train, clogging it. The present method can generate smaller bubbles than available previously. In addition, the bubbles in this paper could be examined simultaneously under an identical impressed sound field, which has potential for comparison, and which increases the rate with which results can be taken.

Comparison of the photographic data with the Rayleigh-Plesset predictions revealed points of discrepancy. In general, the numerical solutions tended to over-estimate the maximum bubble size attained. A bimodal oscillation can occur, which can develop as the bubble size increases towards resonance to produce an oscillation at half the acoustic frequency. For the case illustrated in figure 11 of isothermal bubbles in glycerol (ρ=1260 kg m^{-3}, P_O=333 Pa) the resonance frequencies for bubbles of radius 0.14 mm, 0.19 mm and 0.47 mm are 1010 Hz, 833 Hz and 301 Hz respectively. The data showed a single bubble undergo a change of form oscillation, presumably as a result of a change in R_O through a threshold. The numerical solutions did not show any of these modes developing.

Helium has a large γ and therefore can exhibit a wide range of potential κ. However comparison of Rayleigh-Plesset predictions for bubble in figure 12 showed that the uncertainty in κ cannot account for the observed discrepancies between theory and experiment.

6. CONCLUSIONS

The vertically-vibrating liquid column can accurately simulate an acoustic field in liquid and can generate many interesting features of acoustic cavitation at audio frequencies without the associated hazard to hearing. Comparison of the photographic data with the Rayleigh-Plesset predictions indicates discrepancies. Certain features, such as the occurrence of a bimodal oscillation, were observed photographically but not predicted by the theory for the particular combination of physical parameters. Bimodal behaviour is not uncommon in nonlinear oscillators, and since the actual system studied is more complex than the Rayleigh-Plesset equation assumes (with non-spherical bubbles occurring in clouds) its occurrence for parameters where the theory predicts otherwise is not unexpected.

7. ACKNOWLEDGEMENTS

TGL wishes to thank Magdalene College, Cambridge, and the SERC for Research Fellowships. The authors thank Marconi Maritime for a grant to the laboratory, and for equipment, and Dr. W. J. Fitzgerald for his advice and encouragement. We would like to acknowledge the invaluable assistance of members of the Cavendish Laboratory, particularly C Beton, K Fagan and D Johnson for their computing, photographic and workshop expertise.

8. REFERENCES

[1] Minnaert M. 1933 Phil. Mag., **16**, 235-248
[2] Leighton T G and Walton A J. 1987 Eur. J. Phys., **8**, 98-104
[3] Walton A J and Reynolds G T. 1984 Adv. in Phys., **33**, 595-660
[4] Leighton T G, Wilkinson M, Walton A J and Field J E. 1990. Eur. J. Phys., **11**, 352-358
[5] Crum L A and Hansen G M. 1982. J. Acoust. Soc. Am., **72**, 1586

THE NON-LINEAR OSCILLATIONS OF MULTIPLE BUBBLES IN A SIMULATED ACOUSTIC FIELD.

Figure 10: Comprison of numerical radius/time predictions with photographic data (+) for an air bubble in glycerol, with ρ =1260 kg m^{-3}, P_o =333 Pa, σ = 62.96 mN m^{-1}, P_V =100 Pa, μ=1.49 Pa s , ω =648.6 rad s^{-1}, P_A =3051 Pa, κ =1. a) R_o = 0.24 mm, b) R_o = 0.20 mm .

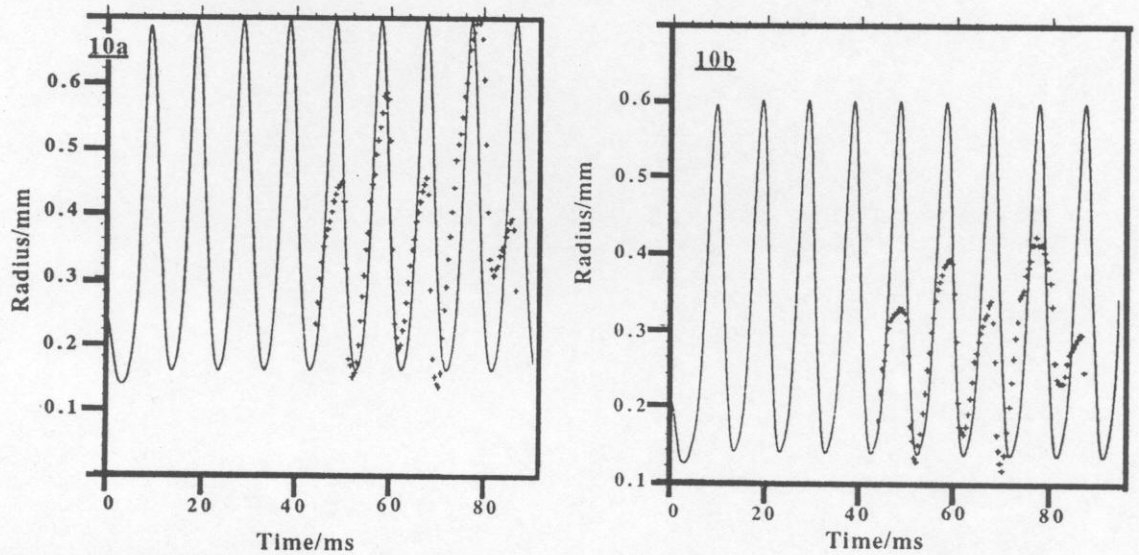

Figure 11: Comprison of numerical radius/time predictions with photographic data (+) for a propane bubble in glycerol, with ρ =1260 kg m^{-3}, P_o =333 Pa, σ = 62.96 mN m^{-1}, P_V =100 Pa, μ=1.49 Pa s, ω =648.6 rad s^{-1}, P_A =3469 Pa, κ =1. a) R_o= 0.14 mm, b) R_o= 0.19 mm, c) R_o= 0.47 mm, d) R_o = 0.47 mm (measured only at t=0).

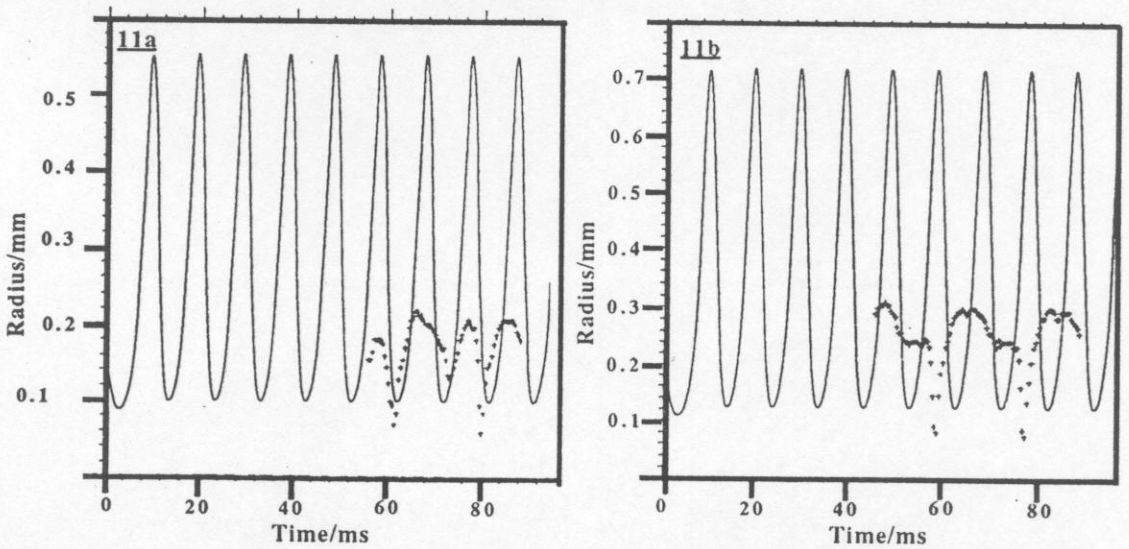

THE NON-LINEAR OSCILLATIONS OF MULTIPLE BUBBLES IN A SIMULATED ACOUSTIC FIELD.

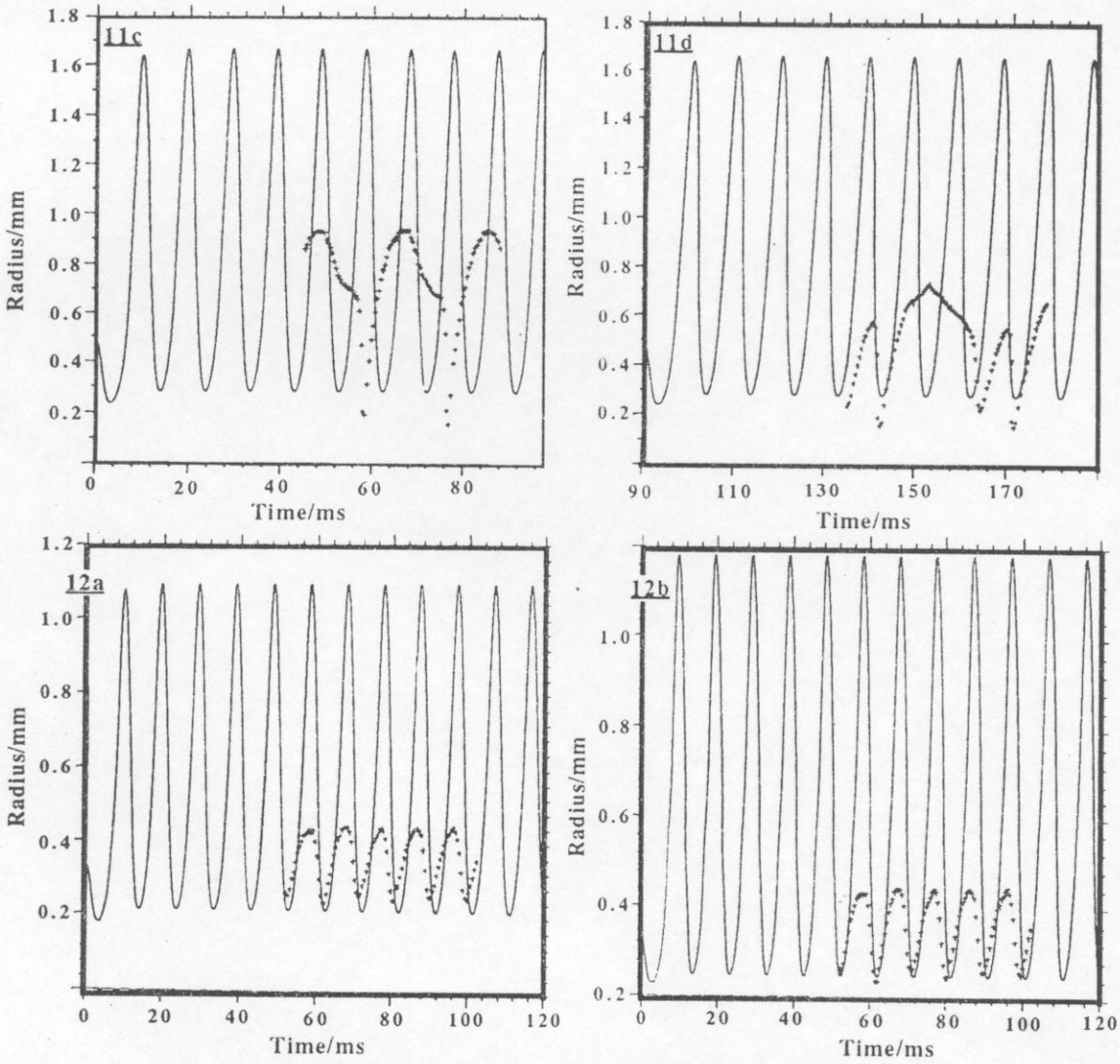

Figure 12: Comprison of numerical radius/time predictions with photographic data (+) for a helium bubble in glycerol, with ρ =1260 kg m $^{-3}$, P_o =333 Pa, σ = 62.96 mN m $^{-1}$, P_v =100 Pa, μ=1.49 Pa s , ω =648.6 rad s $^{-1}$, P_A =3335 Pa, R_o=0.337 mm. a) κ =1, b) $\kappa=\gamma$=1.66